DEUTSCHES ELEKTRONEN – SYNCHROTRON

DESY 92-125
September 1992

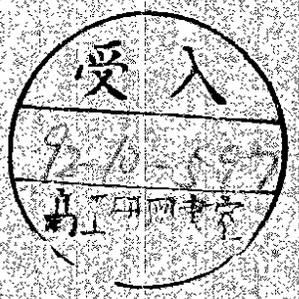

Analysis of the Decay $\tau^- \to \pi^-\pi^-\pi^+\nu_\tau$ and Determination of the $a_1(1260)$ Resonance Parameters

The ARGUS Collaboration

ISSN 0418-9833

NOTKESTRASSE 85 · D-2000 HAMBURG 52

To be sure that your preprints are promptly included in the
HIGH ENERGY PHYSICS INDEX,
send them to (if possible by air mail):

DESY **Bibliothek** **Notkestraße 85** **W-2000 Hamburg 52** **Germany**	**DESY-IfH** **Bibliothek** **Platanenallee 6** **O-1615 Zeuthen** **Germany**

DESY 92-125
September 1992

ISSN 0418-9833

Analysis of the Decay $\tau^- \to \pi^-\pi^-\pi^+\nu_\tau$ and Determination of the $a_1(1260)$ Resonance Parameters

The ARGUS Collaboration

H. Albrecht, H. Ehrlichmann, T. Hamacher, R. P. Hofmann, T. Kirchhoff, A. Nau, S. Nowak[1], H. Schröder, H. D. Schulz, M. Walter[1], R. Wurth
DESY, Hamburg, Germany

R. D. Appuhn, C. Hast, H. Kolanoski, A. Lange, A. Lindner, R. Mankel, M. Schieber, T. Siegmund, B. Spaan, H. Thurn, D. Töpfer, A. Walther, D. Wegener
Institut für Physik[2], Universität Dortmund, Germany

M. Bittner, P. Eckstein
Institut für Kern- und Teilchenphysik[3], Technische Universität Dresden, Germany

M. Paulini, K. Reim, H. Wegener
Physikalisches Institut[4], Universität Erlangen-Nürnberg, Germany

R. Mundt, T. Oest, R. Reiner, W. Schmidt-Parzefall
II. Institut für Experimentalphysik, Universität Hamburg, Germany

W. Funk, J. Stiewe, S. Werner
Institut für Hochenergiephysik[5], Universität Heidelberg, Germany

K. Ehret, W. Hofmann, A. Hüpper, S. Khan, K. T. Knöpfle, J. Spengler
Max-Planck-Institut für Kernphysik, Heidelberg, Germany

D. I. Britton[6], C. E. K. Charlesworth[7], K. W. Edwards[8], E. R. F. Hyatt[6], H. Kapitza[8], P. Krieger[9,7], D. B. MacFarlane[6], P. M. Patel[6], J. D. Prentice[7], P. R. B. Saull[6], K. Tzamariudaki[6], R. G. Van de Water[7], T.-S. Yoon[7]
Institute of Particle Physics[10], Canada

D. Reßing, M. Schmidtler, M. Schneider, K. R. Schubert, K. Strahl, R. Waldi, S. Weseler
Institut für Experimentelle Kernphysik[11], Universität Karlsruhe, Germany

G. Kernel, P. Križan, E. Križnič, T. Podobnik, T. Živko
Institut J. Stefan and Oddelek za fiziko[12], Univerza v Ljubljani, Ljubljana, Slovenia

V. Balagura, I. Belyaev, S. Chechelnitsky, M. Danilov, A. Droutskoy, Yu. Gershtein, A. Golutvin, I. Gorelov, G. Kostina, V. Lubimov, P. Pakhlov, F. Ratnikov, S. Semenov, V. Shibaev, V. Soloshenko, I. Tichomirov, Yu. Zaitsev
Institute of Theoretical and Experimental Physics, Moscow, Russia

[1] DESY, IfH Zeuthen

[2] Supported by the German Bundesministerium für Forschung und Technologie, under contract number 054DO51P.
[3] Supported by the German Bundesministerium für Forschung und Technologie, under contract number 055DD11P.
[4] Supported by the German Bundesministerium für Forschung und Technologie, under contract number 054ER12P.
[5] Supported by the German Bundesministerium für Forschung und Technologie, under contract number 055HD21P.

[6] McGill University, Montreal, Quebec, Canada.

[7] University of Toronto, Toronto, Ontario, Canada.

[8] Carleton University, Ottawa, Ontario, Canada.

[9] Supported in part by the Walter C. Sumner Foundation.
[10] Supported by the Natural Sciences and Engineering Research Council, Canada.
[11] Supported by the German Bundesministerium für Forschung und Technologie, under contract number 054KA17P.
[12] Supported by the Department of Science and Technology of the Republic of Slovenia and the Internationales Büro KfA, Jülich.

Abstract

Using the ARGUS detector at the DORIS II e^+e^- storage ring we have studied the three–pion hadronic final state in the decay $\tau^- \to \pi^-\pi^-\pi^+\nu_\tau$. From about 7500 events we conclude that the three–pion system is dominated by the $J^P = 1^+$ resonance $a_1(1260)$ decaying preferentially via $\rho^0\pi^-$. Our data restrict a possible $\rho\pi$ contribution of three–pion states without intermediate resonances to less than 6% at 95% CL. Fitting a model by Isgur et al. to the data yields $m_{a_1} = (1.211 \pm 0.007 \pm^{0.050}_{0.0})\,\mathrm{GeV/c^2}$ and $\Gamma_{a_1} = (0.446 \pm 0.021 \pm^{0.140}_{0.0})\,\mathrm{GeV/c^2}$. The second errors reflect the model dependence of the result. This is the currently most significant determination of the a_1 resonance parameters. The ratio of S– and D–wave amplitudes for the $\rho^0\pi^-$ intermediate state of the a_1^- decay at the nominal a_1^- mass was found to be $D/S = -0.11 \pm 0.02$. Using this D/S ratio we update our former measurement of the parity violating asymmetry parameter $\gamma_{AV} = 2g_Ag_V/(g_A^2 + g_V^2)$ to $1.25 \pm 0.23 \pm^{0.15}_{0.08}$. The branching ratio of the decay $\tau^- \to \pi^-\pi^-\pi^+\nu_\tau$ is determined to be $\mathrm{Br}(\tau^- \to \pi^-\pi^-\pi^+\nu_\tau) = (6.8 \pm 0.1 \pm 0.5)\%$.

1 Introduction

In the decay $\tau^- \to \pi^-\pi^-\pi^+\nu_\tau$* the weak axial–vector hadronic current can be investigated under very clean conditions. The axial–vector spectral function for the three–pion final state is dominated by the a_1 resonance. Historically, the a_1 resonance, a state with properties consistent with being the P–wave axial–vector $q\bar{q}$ state with isospin I = 1, was finally established in diffractive production from incident π^- [1] and charge–exchange production with low energy π^- [2], both on hydrogen targets. The extraction of the a_1 resonance parameters from these experiments is troubled by the presence of a coherent background, attributed to the Deck effect [3]. Some years later these measurements were confirmed by τ decay data from three different experiments [4,5,6]. The three–pion final state presently offers the best conditions to study the a_1 resonance parameters, the mass and width, and the structure of the a_1 decay [7,8]. An analysis of asymmetries in τ decays to the three–pion final state led to the first observation of parity violation in τ decays and to the determination of the ν_τ helicity [9]. For this study the systematic error was dominated by the uncertainty in the knowledge of the relative D– and S–wave contributions in the $\rho\pi$ intermediate state of the a_1 decay [9,10]. The analysis presented in this paper provides a new measurement of the D/S ratio, allowing an update of the ν_τ helicity determination. This also reduces the systematic uncertainty in the measurement of the normalized product of the weak coupling constant $\gamma_{AV} = 2g_Ag_V/(g_A^2 + g_V^2)$. In order to come to a good understanding of the three–pion final state in τ decays we have also determined the a_1 resonance parameters and the branching ratio for $\tau^- \to \pi^-\pi^-\pi^+\nu_\tau$.

The data for these studies were taken at center–of–mass energies ranging from 9.4 GeV to 10.6 GeV using the ARGUS detector at the electron–positron storage ring DORIS II at DESY. The ARGUS detector is a 4π magnetic spectrometer described in detail elsewhere [11]. The event sample corresponds to an integrated luminosity of about 264 $\mathrm{pb^{-1}}$ which yields about 261 000 produced $\tau^+\tau^-$ pairs.

*References in this paper to a specific charge state imply the charge conjugate state also.

2 Event Selection

We searched for the τ decay into three charged pions by selecting the following combinations of τ decay modes:

$$e^+e^- \longrightarrow \tau^+\tau^- \longrightarrow \pi^-\pi^-\pi^+\nu_\tau$$
$$\hookrightarrow e^-\nu_e\bar{\nu}_\tau\,,\ \mu^-\nu_\mu\bar{\nu}_\tau\,,\ \pi^+ n\gamma\bar{\nu}_\tau \text{ or } K^+ n\gamma\bar{\nu}_\tau,\quad n \geq 0. \quad (1)$$

Events were preselected by requiring exactly four charged tracks with a summed charge of zero. In addition, each charged track had to have a transverse momentum of $p_T > 0.06\,\mathrm{GeV}/c$ and had to point to the main vertex. For this study photons were identified as neutral energy deposits in the electromagnetic calorimeter with energies larger than 0.08 GeV. Since the τ pairs are produced back-to-back with large momenta, their decay products typically point into opposite hemispheres. This characteristic one-versus-three topology was selected by requiring

$$cos(\vec{p}_1, \vec{p}_i) < 0 \quad (i = 2,3,4)$$

and

$$cos(\vec{p}_1, \sum_{i=2}^{4} \vec{p}_i) < -0.5,$$

where $\vec{p}_1$ denotes the momentum of the charged particle on the one-prong side and $\vec{p}_i$ $(i = 2,3,4)$ are the particle momenta on the three-prong side. Photons in the event were only allowed on the one-prong side and thus had to fulfill the condition

$$cos(\vec{p}_1, \vec{p}_\gamma) > 0,$$

with no restriction on the number of photons on the one-prong side. To ensure good momentum resolution and trigger conditions we required the one-prong track to point into the barrel region of the detector, by restricting the polar angle to the region

$$|cos\theta_1| \leq 0.75.$$

To suppress beam-gas and two-photon backgrounds the scalar momentum sum $\sum_{i=1}^{4} |\vec{p}_i|$ was required to be greater than 2.7 GeV/c. Restricting the same quantity to be less than $0.92 \cdot E_{cms}$ suppresses events from exclusive resonance decays, such as $\Upsilon(2S) \to \pi^-\pi^+\Upsilon(1S)$. $\Upsilon(1S) \to l^+l^-$. To suppress further background from QED processes, two-photon reactions and from hadronic processes, we applied the following cut:

$$|\sum_{i=1}^{4} \vec{p}_{Ti}| > (4.5 \cdot (\sum_{i=1}^{4} |\vec{p}_i| \cdot c/E_{cms} - 0.55)^2 + 0.1)\ \mathrm{GeV}/c,$$

where, $\vec{p}_{Ti}$ is the transverse momentum vector of the ith charged particle. Four additional cuts were specifically designed to remove radiative QED backgrounds. First, the energies deposited in the shower counters on the one-prong as well as on the three-prong side both had to be smaller than $0.4 \cdot E_{cms}$. Second, the invariant mass of oppositely-charged particles on the three-prong side, assuming to be electrons, had to be larger than 100 MeV/c^2 to suppress converted photons. Third, the momentum vectors of the one- and three-prong side had to fulfill the condition $\cos(\vec{p}_1, \sum_{i=2}^{4} \vec{p}_i) < -0.999$. Fourth, no particle on the three-prong side was allowed to be identified as an electron.

With these cuts the data sample of about two million events is reduced to 10 606 events. Of those a subset of 10 323 events have an invariant mass of the three-pion system of less than 1.8 GeV/c.

3 Background Determination

The selected data sample still contains background events from the following sources:

- two-photon reactions,
- radiative QED events with converted photons,
- e^+e^- annihilation into hadrons,
- other τ decay modes, in particular $\tau^- \to \pi^-\pi^-\pi^+\pi^0\nu_\tau$.

In the following the separate background channels and their determination will be dicussed in detail. Their absolute contributions to the selected events are listed in table 1.

	events
selected events	$10\,323 \pm 102$
background channel	
$\tau^- \to \pi^-\pi^-\pi^+\pi^0\nu_\tau$	$1\,422 \pm 179$
$\tau^- \to K^-\pi^-\pi^+\nu_\tau$	276^{+202}_{-164}
$\tau^- \to K^-K^+\pi^-\nu_\tau$	261^{+203}_{-132}
$\tau^- \to K^*(892)^-\nu_\tau$	48^{+7}_{-8}
$e^+e^- \to q\bar{q}$	744 ± 90
$e^+e^- \to e^+e^-X$	15 ± 8
$e^+e^- \to l^+l^-\gamma$	80 ± 20
total background	2846^{+350}_{-292}

Table 1: Number of selected events and background contributions.

Background from two-photon reactions

The background from two-photon reactions $e^+e^- \to e^+e^-X$ was studied by Monte Carlo simulation. The main sources considered were the two-photon production of the $\pi^-\pi^-\pi^+\pi^+$ and $\pi^-\pi^-\pi^+\pi^+\pi^0$ final states. Events were generated in the two-photon invariant mass range $0.5\,\mathrm{GeV}/c^2 < W_{\gamma\gamma} < 4\,\mathrm{GeV}/c^2$ with a constant cross section for $\sigma_{\gamma\gamma\to X}(W_{\gamma\gamma}) = 1\,\mathrm{nb}$. Since the exact fraction and $W_{\gamma\gamma}$ distribution of two-photon events in our data sample is not known, the weight of the simulated events was adjusted to match the data by the following procedure. First the cuts which suppress the background from two-photon reactions were inverted, i.e. events were required to satisfy:

- $\sum_{i=1}^{4} \vec{p}_{Ti} < (4.5 \cdot (\sum_{i=1}^{4} |\vec{p}_i| \cdot c/E_{cms} - 0.55)^2 + 0.1)\ \mathrm{GeV}/c$

- and $\sum_{i=1}^{4} |\vec{p}_i| < 2.7$ GeV/c.

All other cuts remained unchanged. Then, comparing the four-pion mass distribution of the simulated events and the data, we derived weighting factors as a function of the four-pion mass. Finally, the simulated background events from two-photon reactions which passed the selection criteria for reaction (1) were normalized by applying the weighting factors. This method yields 15 ± 8 background events from two-photon reactions.

Background from radiative QED events

The applied cuts have been very efficient in removing the background from radiative QED events with converted photons. The remaining background from this source was determined from data itself by studying events with reconstructed converted photons. Given our selection criteria, this background contribution is found to be 80 ± 20 events.

Background from one-photon annihilation into hadrons

The distribution of invariant three-pion masses in fig. 1 exhibits a tail above the τ mass which indicates remaining background from one-photon annihilation into hadrons. The contribution from two-photon processes in this mass range was found to be negligible. The possible background sources from one-photon annihilation are:

- Annihilation of e^+e^- pairs into quark-antiquark pairs, with possible initial-state radiation:

$$e^+e^- \to q\bar{q}(\gamma)\,.$$

- Υ decays into three gluons and Υ decays into two gluons and one photon, where the latter is suppressed by a factor of $\alpha/\alpha_s \approx 0.05$ [12]:

$$\Upsilon \to ggg \text{ und } \Upsilon \to gg\gamma\,.$$

- $\Upsilon(4S)$ decays into a pair of B mesons. A simulation for this reaction shows that less than five events with a three pion mass below the τ mass contribute to the selected data sample.

For the background determination only the $q\bar{q}(\gamma)$ process was simulated since the expected contribution from Υ decays into three gluons is only 10% of the former and the three pion mass spectra of these two background sources differ only slightly.

The LUND Monte Carlo program (version 6.2 and 6.3) [13] was used to generate 711 570 $q\bar{q}(\gamma)$ events, a good match to the estimate, based on the integrated luminosity and the known cross section, of 870 000 $q\bar{q}(\gamma)$ events in the data. In the three-pion mass range between 2 GeV/c^2 and 4 GeV/c^2, 164 and 133 events were found in the data and the simulation, respectively. The ratio of events in this mass range (1.23) is in exellent agreement with the ratio of the initial Monte Carlo and data sample sizes (1.22). In fig. 1 the measured three-pion mass distribution is compared to the normalized distribution from the simulation. Both spectra agree very well above the τ mass, giving some confidence in the extrapolation into the region populated by τ events. Below the τ mass ($m_{3\pi} < 1.8 GeV$) 744 ± 90 events are estimated to remain from hadronic one-photon events.

Background from other τ decay modes

Four different τ decays contribute to this source: (a) $\tau^- \to \pi^-\pi^-\pi^+\pi^0\nu_\tau$, (b) $\tau^- \to K^-\pi^-\pi^+\nu_\tau$, (c) $\tau^- \to K^-K^+\pi^-\nu_\tau$ and (d) $\tau^- \to K^{*-}\nu_\tau$ decays. As noted in table 1 the largest contribution arises from τ decays into three charged pions and one π^0 where the photons of the π^0 decay escape detection. Therefore this channel has been given particularly careful treatment. The number of events from channel (a) contributing to the selected data was determined by a Monte Carlo simulation using a branching ratio of $(5.4 \pm 0.4 \pm 0.5)\%$ as measured by ARGUS [14]. The simulation took into account the measured subresonance structure of the four-pion final state [15]. In this way 1422 ± 179 events of channel (a) were found to contribute to our data sample.

The shape of the three-pion mass distribution from the dominant background channel (a) is most crucial for the systematic uncertainties in the determination of the a_1 resonance parameters. In order not to rely on the Monte Carlo simulation on this point we proceeded as follows. First the three-pion mass distribution was determined for events from channel (a) where the π^0 was detected. This was achived by applying the same selection criteria as for reaction (1) with the exception that two photons with an invariant mass consistent with the π^0 mass, were required on the three-prong side. The spectrum obtained has to be also corrected for background. Contributions from two-photon reactions, radiative QED events and from other τ decays were found to be negligible. The background from one-photon annihilation into hadrons was determined as described for the three-pion final state using in this case the four-pion mass distribution for normalization.

The three-pion mass distribution depends on whether the the π^0 is detected or not. This change was determined as a function of the three-pion mass using the Monte Carlo simulation. Appyling this correction function to the measured three-pion mass distribution in events with detected π^0's and normalizing this distribution to the numbers predicted by the Monte Carlo, we obtain a three-pion mass distribution for background (a), which was subtracted from the selected data of reaction (1). All other distributions which will be used below were corrected in a similar fashion.

The background contribution from reaction (b), (c) and (d) were determined using world average branching ratios [16] (table 2). The τ decays (b) and (c) were always assumed to proceed through a short-lived, heavy intermediate resonance. In particular, the $KK\pi$ final state was simulated using the channel $\tau^- \to \rho(1700)^-\nu_\tau$ followed by a phase space decay of the $\rho(1700)$ into $KK\pi$. The parameters for the $\rho(1700)$ mass distribution were adjusted to fit the measured $\pi^-\pi^-\pi^+\pi^0$ mass distribution [15]. To simulate the $K\pi\pi$ final state we generated the decays $\tau^- \to K_1(1270)^-\nu_\tau$ and $\tau^- \to K_1(1400)^-\nu_\tau$. Since the relative contributions of these resonances to τ decays to the $K\pi\pi$ final state are not known, they are assumed to be equal. The background contribution from reaction (d) was determined by simulating the decay $K^{*-} \to K_s^0\pi^-$.

The three-pion invariant mass distribution of the selected events, together with the sum of the background contributions, is shown in fig. 2. Figure 3 shows the invariant $\pi^-\pi^+$ and $\pi^-\pi^-$ mass distribution before background subtraction. The background is subtracted from all distributions shown below.

decay channel	branching ratio [16]
three–prong	
$\tau^- \to \pi^-\pi^-\pi^+\pi^0\nu_\tau$	$(5.40 \pm 0.64)\%$ [14]
$\tau^- \to K^-\pi^-\pi^+\nu_\tau$	$(0.22\pm^{0.16}_{0.13})\%$
$\tau^- \to K^-K^+\pi^-\nu_\tau$	$(0.22\pm^{0.17}_{0.11})\%$
$\tau^- \to K^*(892)^-\nu_\tau$	$(0.31 \pm 0.04)\%$
one–prong	
$\tau^- \to e^-\bar{\nu}_e\nu_\tau$	$(17.8 \pm 0.4)\%$
$\tau^- \to \mu^-\bar{\nu}_\mu\nu_\tau$	$(17.7 \pm 0.4)\%$
$\tau^- \to \pi^-\nu_\tau$	$(11.0 \pm 0.5)\%$
$\tau^- \to \rho^-\nu_\tau$	$(22.7 \pm 0.8)\%$
$\tau^- \to a_1^-\nu_\tau$	$(7.5 \pm 0.9)\%$
$\tau^- \to \pi^- 3\pi^0\nu_\tau$	$(3.0 \pm 2.7)\%$
$\tau^- \to K^-\nu_\tau$	$(0.68 \pm 0.19)\%$
$\tau^- \to K^*(892)^-\nu_\tau$	$(1.08 \pm 0.15)\%$
$\sum_{one-prong}$	81.46%

Table 2: Branching ratios used in the Monte Carlo simulations. Also for the simulation the sum of the one–prong exclusive modes was scaled to the topological branching ratio of 86.13%.

4 Acceptance Calculation

The acceptance for the decay $\tau^- \to \pi^-\pi^-\pi^+\nu_\tau$ was determined by a Monte Carlo simulation of the detector [17] using the KORALB [18] event generator, which takes the effect of initial–state radiation into account. In KORALB the a_1 parameters were adjusted to $m_{a_1} = 1280\,\mathrm{MeV/c^2}$ and $\Gamma_{a_1} = 599\,\mathrm{MeV/c^2}$. In table 2 the one–prong branching ratios used to generate the events are listed. We factorized the total efficiency η in the following way:

$$\eta = \eta_{selection} \times \eta_{trigger} \times \eta_\gamma$$

where $\eta_{selection}$ is the efficiency for event reconstruction and the selection criteria, $\eta_{trigger}$ the trigger efficiency and η_γ the efficiency due to the photon cuts. The trigger simulation uses different trigger thresholds for different data taking periods and adds the trigger probability as a weighting factor to the event record of the simulated events. The efficiency η_γ describes the losses from the requirement that no photons are allowed on the three–prong side due to noise or misidentified clusters in the electromagnetic calorimeter. The probability to find faked photons in an event was determined using cosmic, as well as randomly triggered events, leading to consistent results. As shown in fig. 4 and 5 background subtracted three–pion and two–pion mass distributions are well reproduced by the KORALB Monte Carlo program. With $\eta_{selection} = 0.274 \pm 0.014$, $\eta_{trigger} = 0.971 \pm 0.003$ and $\eta_\gamma = 0.917 \pm 0.005$ the overall efficiency was determined to be $\eta = 0.244 \pm 0.013$. Within the statistical accuracy of the Monte Carlo simulation no dependence of the acceptance on the three– and two–pion masses was found.

5 Analysis of the Three–Pion Final State

The three–pion final state in τ decays is known to be dominated by the $a_1(1260)$ resonance which in turn almost exclusively decays via a $\rho\pi$ intermediate state [6]. Hence, the selected three–charged–pion final state is expected to originate mostly from the decay chain:

$$\tau^- \to a_1^-\nu_\tau \to \rho^0\pi^-\nu_\tau \to \pi^-\pi^-\pi^+\nu_\tau. \qquad (2)$$

In the analysis of the three–pion final state and the determination of the a_1 resonance parameters we had to study the following questions:

- Is there non–resonant three–pion background to reaction (2)?
- Are there other than $\rho\pi$ intermediate states in reaction (2), such as $(\pi\pi)_{S-wave}\pi$, where the $\pi\pi$ S–wave state may or may not form a resonance?
- Is the $\rho\pi$ system in a relative S– or D–wave state?

The description of a broad resonance is known to be notoriously difficult and in general the determination of the resonance mass and width becomes model dependent. To be definit, we have chosen to perform the analysis on the basis of the model of Isgur, Morningstar and Reader [8]. It contains various a_1 decay channels, including the effect on the three–pion channel of the opening of the K^*K threshold, and a possible non–resonant background. Apart from being quite sophisticated, this model had the advantage to be available for detailed fits to the data [19]. The model dependence of the results will also be discussed.

5.1 Two Pion Mass Distributions and Dalitz Plot Analysis

Figure 3 shows the invariant $\pi^-\pi^+$ mass distribution together with the invariant $\pi^-\pi^-$ mass distribution before background subtraction. The $\pi^-\pi^+$ spectrum shows, in addition to the expected ρ resonance, a clear enhancement in the mass region of the K^0 meson. The K^0 mesons are due to background events from $K\bar{K}\pi$, $K\pi\pi$ and $K^*(892)$ decays of the τ. Comparing the number of K^0 mesons in the invariant $\pi^-\pi^+$ mass spectrum of the data with the corresponding number from the background simulation allows a check of the background determination at least for these three sources. Fitting a gaussian to the K^0 signals yields 137 ± 37 candidates in the data sample, in good agreement with the $125\pm^{41}_{27}$ K^0 candidates from the simulated background events. The background subtracted $\pi^-\pi^+$ and $\pi^-\pi^-$ invariant mass distributions are displayed in fig. 5 together with the results of the simulation. The $\pi^-\pi^+$ distribution shows the ρ resonance on top of a smooth background. Visible is a slight shift of about $10 - 15\,\mathrm{MeV/c^2}$ of the resonance with respect to the simulation. The Monte Carlo program [18] uses a resonance parametrization which is found to describe the ρ resonance in the decay $\tau^- \to \rho^-\nu_\tau$ [20] with $m_\rho = 0.773\,\mathrm{GeV/c^2}$ and $\Gamma_\rho = 0.143\,\mathrm{GeV/c^2}$. The origin for this small discrepancy in the three–pion data could not be found. It is possible that final state interactions modify the resonance shape.

The non–resonant background in the $\pi^-\pi^+$ spectrum is roughly accounted for by the like–sign combination. This shows the dominance of the $\rho\pi$–channel while the non–resonant $\pi^-\pi^+$ background is just described by the wrong mass combination. Looking closer, however, one finds some indication that the $\pi^-\pi^-$ distribution exceeds the $\pi^-\pi^+$ distribution at low masses.

Such a behaviour is expected if the two possible $\pi^-\pi^+$ combinations interfere constructively, both preferring to be in the ρ-state and thereby reducing the phase space left for the $\pi^-\pi^-$ combination. The two-pion mass spectrum is also influenced by the relative angular momenta in the three-pion system. More complete information is contained in the Dalitz plot of the three-pion system which will be discussed below.

5.2 Dalitz Plot Analysis

The D and S wave contributions in the decay $a_1 \to \rho\pi$ were determined by studying the Dalitz plots of the three-pion system in different three-pion mass bins. In fig. 6 the Dalitz plot densities for four intervals of the three-pion mass are shown, where $s_1 = (p_{\pi_2^-} + p_{\pi^+})^2 = m^2_{\pi_2^-\pi^+}$ and $s_2 = (p_{\pi_1^-} + p_{\pi^+})^2 = m^2_{\pi_1^-\pi^+}$. Cutting out the mass bands around the ρ for one $\pi^-\pi^+$ combination and projecting the band onto the other $\pi^-\pi^-$ axis yields the Dalitz plot projections shown in fig. 6 on the right side. Fitting these plots with the Isgur et al. model [8] yields an amplitude ratio

$$\mathrm{D/S} = -0.11 \pm 0.02$$

in good agreement with the prediction D/S $= -0.15$ from a 'flux tube breaking' model [8]. The D/S ratio holds for the nominal a_1 mass and has a mass dependence given by the model, including for example the different threshold behaviour for S and D waves. The results are consistent with those obtained using the model of Feindt [22] which contains no additional mass dependence in the couplings. In fig. 6 the data are well fitted by the model, except for the three-pion mass bin between 1.0 and 1.2 GeV/c^2. Here further investigations are necessary to determine, for example, whether the amplitudes are modified by final state interactions. Due to these uncertainties it is hard to estimate a systematic error for this result. Therefore we give the statistical error of the fit only.

The dominance of the $\rho\pi$ mode can be established from a study of the two-pion invariant mass distributions. The distributions of the $\pi^-\pi^+$ and $\pi^-\pi^-$ masses are shown in fig. 5. To determine a possible non-$\rho\pi$ resonance contribution in the final state we proceeded as follows. First we generated a $\pi^-\pi^+$ invariant mass spectrum using a Monte Carlo for an D/S ratio of -0.11 assuming $\rho\pi$ dominance. Second we generated the $\pi^-\pi^+$ invariant mass spectrum for a pure a_1 phase space decay. Fitting the $\pi^-\pi^+$ and $\pi^-\pi^-$ spectra simultaneously with the sum of the two contributions, we estimate that the non-$\rho\pi$ contribution to the $\pi^-\pi^-\pi^+$ final state is less than 6.0% at the 95% CL. We want to stress that this limit holds only for this particular model. A more general approach seems not to be possible, given the lack of understanding of, for example, final state interactions.

5.3 Analysis of the Three–Pion Invariant Mass Distribution

For the determination of the mass and width of the a_1 resonance the model of Isgur, Morningstar and Reader [8] was used. In the parametrization of the model the measured D/S ratio was used. Further, it was assumed that $\rho\pi$ was the only contribution to the three-pion final state of the a_1 decay but K^*K was allowed to contribute to the total a_1 width. The $\pi(1300)$ resonance was considered as the only other possible significant contribution to the three-pion final state, although the model predicts this contribution is small [23]. Therefore this contribution was not included in the fit. The fit took account of possible non-a_1 contributions by a three-parameter polynomial. Since the fit yielded an insignificant background of this type

and the data were well described by the fit, we conclude that the model contains all essential features needed to describe the data. Furthermore, the determination of the a_1 parameters was insensitive to whether a background term was included or not. The fit result, together with the background subtracted and acceptance corrected three-pion mass distribution, is shown in fig. 7. The fitted results on the a_1 resonance parameters are:

$$\begin{aligned} m_{a_1} &= (1.211 \pm 0.007)\,\mathrm{GeV}/c^2 \\ \Gamma_{a_1} &= (0.446 \pm 0.021)\,\mathrm{GeV}/c^2. \end{aligned}$$

Table 3 shows that these values are consistent with those obtained by the authors of [8] for DELCO [4] and Mark II [5] data. However, the ARGUS results have by far the smallest statistical errors. In addition, the new result is in good agreement with our previous measurement [6]. Table 4 shows the a_1 parameters determined from fitting different models to the ARGUS data. Bowler and Törnqvist both use relativistic Breit–Wigner formulas to describe the three-pion mass distribution. Törnqvist in addition considers the K^*K threshold effects. While the mass values vary only by 50 MeV/c^2, the spread of about 140 MeV/c^2 in the width is quite large. In hadronic reactions (also shown in table 4) the width is found to be smaller. However, Bowler finds that, with an alternative parametrization of the Deck amplitude, the hadronic data can be made consistent with the τ data [16,24].

Experiment	m_{a_1}(GeV/c^2)	Γ_{a_1}(GeV/c^2)
ARGUS new	1.211 ± 0.007	0.446 ± 0.021
DELCO*	1.180 ± 0.060	0.430 ± 0.190
MARK II*	1.250 ± 0.050	0.580 ± 0.100
ARGUS 86*	1.213 ± 0.011	0.434 ± 0.030

Table 3: Comparison of mass and width of the a_1 meson for different experiments using the Isgur et al. model [8]. The starred results are taken from [8].

Model	Ref.	m_{a_1}(GeV/c^2)	Γ_{a_1}(GeV/c^2)	χ^2/NDF
Isgur et al.	[8]	1.211 ± 0.007	0.446 ± 0.021	16.5/22
Bowler	[7]	1.236 ± 0.006	0.450 ± 0.022	78.1/36
Kühn et al.	[20]	1.274 ± 0.007	0.594 ± 0.023	46.8/36
Ivanov et al.	[26]	1.246 ± 0.006	0.483 ± 0.021	55.1/36
Törnqvist	[27]	1.224*	0.592*	
$\pi^- p \to \pi^-\pi^-\pi^+ p$	[1]	1.280 ± 0.030	0.300 ± 0.050	
$\pi^- p \to \pi^-\pi^+\pi^0 n$	[2]	1.240 ± 0.080	0.380 ± 0.100	

Table 4: Results for the a_1 parameters from ARGUS using different models and from hadronic reactions. (* The fit of Törnqvist still uses the old ARGUS data.)

In addition to the mass spectrum $dN/dm_{3\pi}$, we show in fig. 8 the spectral density $\rho_t(Q^2)$ (with $Q^2 = m^2_{3\pi}$), defined by [25]:

$$\frac{d\Gamma_{3\pi\nu}(Q^2)}{dQ^2} = \frac{G_F^2 cos^2\Theta_c}{16\pi m_\tau^3}(m_\tau^2 - Q^2)^2\{(m_\tau^2 - 2Q^2)\rho_t(Q^2) + m_\tau^2\rho_l(Q^2)\}$$

where ρ_t and ρ_l are the transverse and longitudinal components of the spectral density. According to this formula we derived ρ_t from fig. 7 neglecting the contribution of ρ_l, which is of the order m_π^2/Q^2 under the assumption of PCAC.

5.4 Update on Parity Violation in Tau Decays

If the new measurement of the D/S ratio were used, the systematic uncertainty in the determination of the parameter γ_{AV} which describes the parity violating asymmetry [9,22], could be significantly reduced. Since the selection criteria used here have a higher efficiency than those for our previous publication [9] the statistical error on γ_{AV} is also reduced. The new result obtained for γ_{AV} is:

$$\gamma_{AV} = \frac{2g_A g_V}{g_A^2 + g_V^2} = 1.25 \pm 0.23 \pm^{0.15}_{0.08}.$$

The asymmetry as a function of the squared three-pion mass $Q^2_{3\pi}$ is shown in fig. 9. With our sign convention the Standard Model yields $\gamma_{AV} = +1$ for left-handed tau neutrinos, in good agreement with our measurement.

6 Determination of the τ Decay Branching Ratio

The investigation of the two- and three-pion mass distribution described in the previous section confirms that our Monte Carlo simulation is well suited to describing τ decays into three pions. We can therefore use the efficiency determined in section 4 to calculate the branching ratio, using the formula:

$$BR(\tau^- \to \pi^-\pi^-\pi^+\nu_\tau) = \frac{1}{\eta \cdot BR_1} \cdot \frac{N_{sel} - N_{bg}}{2 \cdot N_{\tau\tau}}.$$

The number of produced τ pairs $N_{\tau\tau} = 261\,485 \pm 860 \pm 5\,364$, which enters into the determination of the branching ratio, was calculated using the cross section of continuum τ pair production including radiative processes up to order α^3. The relative systematic error on this number is estimated to be less than 1% [28]. For the data taken on the $\Upsilon(1S)$ and $\Upsilon(2S)$ resonances the number of τ pairs was scaled to include the enhancement due to vacuum polarisation. These contributions were determined from the visible hadronic cross section ad DORIS II of 9.1 nb for the $\Upsilon(1S)$ and 3.3 nb for the $\Upsilon(2S)$ resonance, and the branching ratio $BR(\Upsilon \to \tau^-\tau^+)$. Assuming lepton universality the later was obtained from the more accurately measured branching ratios $BR(\Upsilon(1S) \to \mu^-\mu^+) = (2.75 \pm 0.07)\%$ and $BR(\Upsilon(2S) \to \mu^-\mu^+) = (1.37 \pm 0.26)\%$ [16]. The radiative tail of the Υ resonances was not taken into account but the effect was estimated to be smaller than 0.1%. The number of selected events, N_{sel}, and background events N_{bg} are listed in table 1; the efficiency

$\eta = 0.244 \pm 0.013$ was discussed in section 4, while for the one-prong branching ratio we used $BR_1 = (86.13 \pm 0.33)\%$. Thereby we obtain:

$$BR(\tau^- \to \pi^-\pi^-\pi^+\nu_\tau) = (6.8 \pm 0.1 \pm 0.5)\%$$

where the first error is due to the statistical uncertainty on the number of selected events. The second error is due to systematic uncertainties in the Monte Carlo determination of the efficiencies, the luminosity measurement which enters into the number of τ pairs, the one-prong branching ratio and the branching ratios used for background subtraction.

7 Conclusion

In conclusion we have measured the parameters of the $\pi^-\pi^-\pi^+$ final state in τ decays. The decay is dominated by the a_1 resonance which decays via a $\rho\pi$ intermediate state into three pions. We found that the non-$\rho\pi$ contribution to the a_1 decay is less than 6% at the 95% CL where final-state interactions were not taken into account. The ρ and π are dominantly in a S-wave state with a small D-wave contribution. The ratio of S- and D-wave amplitudes at the nominal a_1 mass was determined to be

$$D/S = -0.11 \pm 0.02$$

using the Isgur et al. model [8]. Fitting the same model to the three-pion mass distribution yields the following values for the mass and width of the a_1:

$$m_{a_1} = (1.211 \pm 0.007)\,GeV/c^2$$
$$\Gamma_{a_1} = (0.446 \pm 0.021)\,GeV/c^2.$$

Other resonance and non-resonant background is not required by the fit. Using the measured D/S value we update our measurement of the parity violating asymmetry parameter γ_{AV} to

$$\gamma_{AV} = \frac{2g_A g_V}{g_A^2 + g_V^2} = 1.25 \pm 0.23 \pm^{0.15}_{0.08}.$$

Finally we determined the τ decay branching ratio $Br(\tau^- \to \pi^-\pi^-\pi^+\nu_\tau) = (6.8 \pm 0.1 \pm 0.5)\%$. This result supersedes that published earlier by the ARGUS group [6]. Taking into account that other experiments do not subtract the background contributions from τ decays into three charged particles where one or two of the particles are kaons, our result is in statistical agreement with the measurements of MARK II [5] and MAC [29] and in disagreement with the measurements of ALEPH [30] and CELLO [31].

Acknowledgements

It is a pleasure to thank U. Djuanda, E. Konrad, E. Michel, and W. Reinsch for their competent technical help in running the experiment and processing the data. We thank Dr. H. Nesemann, B. Sarau, and the DORIS group for the excellent operation of the storage ring. The visiting groups wish to thank the DESY directorate for the support and kind hospitality extended to them. We want to thank Dr. C. Reader, Dr. M. Feindt and Dr. J.H. Kühn for helpful discussions about the theoretical framework of this measurement.

References

[1] C.Daum et al., Nucl. Phys. **B182** (1981) 269.

[2] J.Dankowych et al., Phys. Rev. Lett. **46** (1981) 580.

[3] R.T.Deck, Phys. Rev. Lett. **13** (1964) 169.

[4] W.Ruckstuhl et al. (DELCO Collaboration), Phys.Rev.Lett. **56** (1986) 2132.

[5] W.B.Schmidke et al. (MARK II Collaboration), Phys.Rev.Lett. **57** (1986) 527.

[6] H.Albrecht et al. (ARGUS Collaboration), Z.Phys. **C33** (1986) 7.

[7] M.G.Bowler, Phys. Lett. **182B** (1986) 400.

[8] N.Isgur, C.Morningstar and C.Reader, Phys.Rev. **D39** (1989) 1357.

[9] H.Albrecht et al. (ARGUS Collaboration) Phys.Lett. **B250** (1990) 164.

[10] A.Walther, *'Study of the Decay $\tau^- \to \pi^-\pi^-\pi^+\nu_\tau$ and Determination of the Tau-Neutrino Helicity'*, doctoral thesis (in German), University of Dortmund, 1991.

[11] H.Albrecht et al. (ARGUS Collaboration), Nucl. Instrum. Methods **A275** (1989) 1.

[12] H.Albrecht et al. (ARGUS Collaboration), Phys. Lett. **199B** (1987) 291.

[13] B.Andersson et al., Phys. Rep. **97** (1983) 31; Phys. Lett. **199B** (1987) 291.

[14] A.Krüger, doctoral thesis (in German). University of Hamburg. DESY internal note, **DESY F15-91-03** (1991).

[15] H.Albrecht et al. (ARGUS Collaboration), Phys. Lett. **260B** (1991) 259.

[16] Particle Data Group, Phys. Lett. **239B** (1990) 1.

[17] H.Gennow, "SIMARG: A Program to simulate the ARGUS Detector". DESY internal note, DESY **F15-85-02** (1985).

[18] S.Jadach and Z.Was, "Monte Carlo simulation of the process $e^+e^- \to \tau^+\tau^-, \tau^\pm \to X^\pm$ including radiative $\mathcal{O}(\alpha^3)$ QED corrections, mass and spin effects", Comp. Phys. Comm. **36** (1985) 191;
S.Jadach and Z.Was, "KORALB version 2.1 – An upgrade with TAUOLA library of τ decays", CERN-TH-5855/90;
S.Jadach, J.H.Kühn and Z.Was, "TAUOLA version 1.5 – A library of Monte Carlo programs to simulate decays of polarized τ leptons", CERN-TH-5856/90.

[19] The fits have been carried out by C.Reader and C.Morningstar.

[20] J.H.Kühn and A.Santamaria, Z. Phys. **C 48** (1990) 445.

[21] J.H.Kühn, F.Wagner, Nucl. Phys. **B236** (1984) 16.

[22] M.Feindt, Z.Phys. **C48** (1990) 681.

[23] C.Reader private communication.

[24] M.G.Bowler, Phys. Lett. **209B** (1988) 99.

[25] L.B.Okun, "Leptons and Quarks", Amsterdam North-Holland (1982).

[26] M.K.Volkov, Yu.P.Ivanov, A.A.Osipov, Z. Phys. **C49** (1991) 563.

[27] N.A.Törnqvist, Z. Phys. **C36** (1987) 695.

[28] F.A.Berends and R.Kleiss, Nucl. Phys. **B177** (1981) 237.
F.A.Berends and R.Kleiss, Nucl. Phys. **B178** (1981) 141.

[29] H.Band et al. (MAC Collaboration), Phys. Lett. **198B** (1987) 297.

[30] D.Decamp et al. (ALEPH Collaboration), Z. Phys. **C 54** (1992) 75.

[31] H.J.Behrend et al. (CELLO Collaboration), Z. Phys. **C46** (1990) 537.

[32] H.Albrecht et al. (ARGUS Collaboration), Z. Phys. **C53** (1992) 367.

Figure captions

1. Three–pion mass spectrum of the selected events together with the $m_{3\pi}$ spectrum of the hadronic background (shaded histogram). In the right upper corner the mass region between 1.6 GeV/c^2 and 3.0 GeV/c^2 is shown with an expanded scale.

2. Three–pion mass distribution: the shaded area indicates the total background.

3. Invariant $\pi^-\pi^+$ (full points) mass distribution together with the invariant $\pi^-\pi^-$ mass distribution before background subtraction.

4. Background corrected three–pion mass distribution together with the Monte Carlo simulation (histogram).

5. Background and acceptance corrected two–pion mass distribution together with the Monte Carlo simulation (Full lines).
   Full points: $\pi^-\pi^+$ (two entries per event)
   Histogram with error bars: $\pi^-\pi^-$.

6. Dalitz plots and projections for the decay $\tau^- \to \pi^-\pi^-\pi^+\nu_\tau$ for four three–pion mass intervals. From top to bottom,
   $0.8\,\mathrm{GeV}/c^2 \le m_{3\pi} < 1.0\,\mathrm{GeV}/c^2$,
   $1.0\,\mathrm{GeV}/c^2 \le m_{3\pi} < 1.2\,\mathrm{GeV}/c^2$,
   $1.2\,\mathrm{GeV}/c^2 \le m_{3\pi} < 1.4\,\mathrm{GeV}/c^2$,
   $1.4\,\mathrm{GeV}/c^2 \le m_{3\pi} < 1.6\,\mathrm{GeV}/c^2$.
   The curves in the Dalitz plots are the Dalitz plot boundaries for the specific upper boundery of the three–pion mass interval. The included bounderies of the ρ bands are at $(m_\rho \pm 65\,\mathrm{MeV}/c^2)^2$. The curves in the Dalitz plot projections are the results of a fit to the Isgur et al. model [8].

7. Background subtracted and acceptance corrected three–pion mass distribution fitted with the model of Isgur et al. (dotted line: polynomial background used in the fit). This distribution is tabulated in the appendix in table 5.

8. Distribution of the axial–vector spectral density $\rho_t(Q^2)$ determined for the decay $\tau^- \to \pi^-\pi^-\pi^+\nu_\tau$, under the assumption that $\rho_t(Q^2) = 0$. (With $\Gamma_{e\nu\bar{\nu}} = (17.30 \pm 0.40 \pm 0.50)\%$) as measured by ARGUS [32]). This distribution is tabulated in the appendix in table 7.

9. The parity violating asymmetry as a function of the square of the three–pion mass (curve: prediction for $\gamma_{A1} = +1.25$). The values of this asymmetry are tabulated in the appendix in table 6.

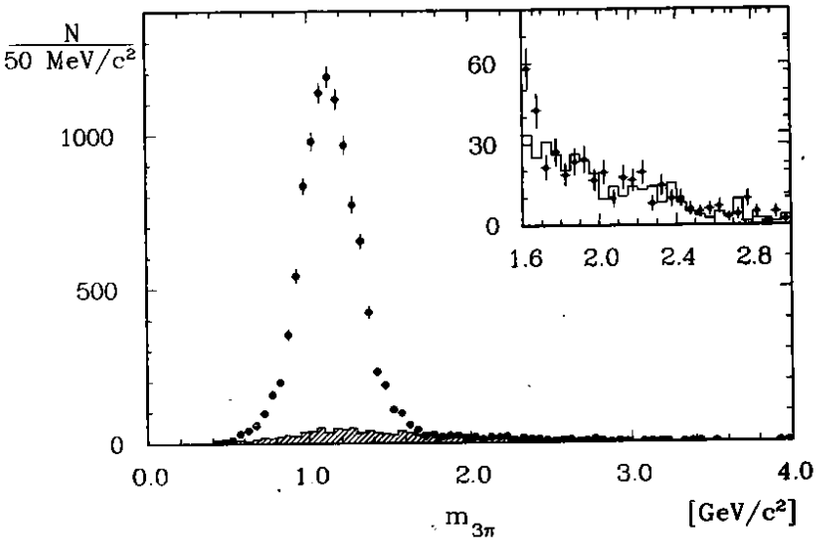

Figure 1

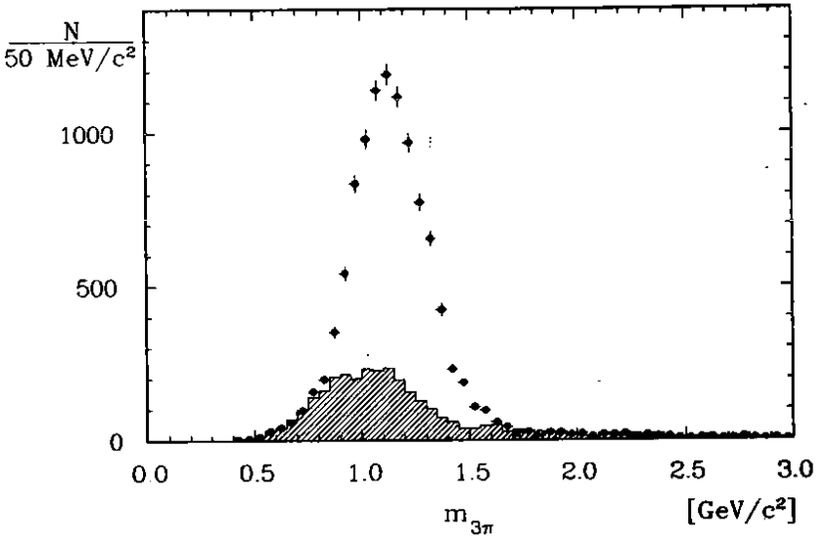

Figure 2

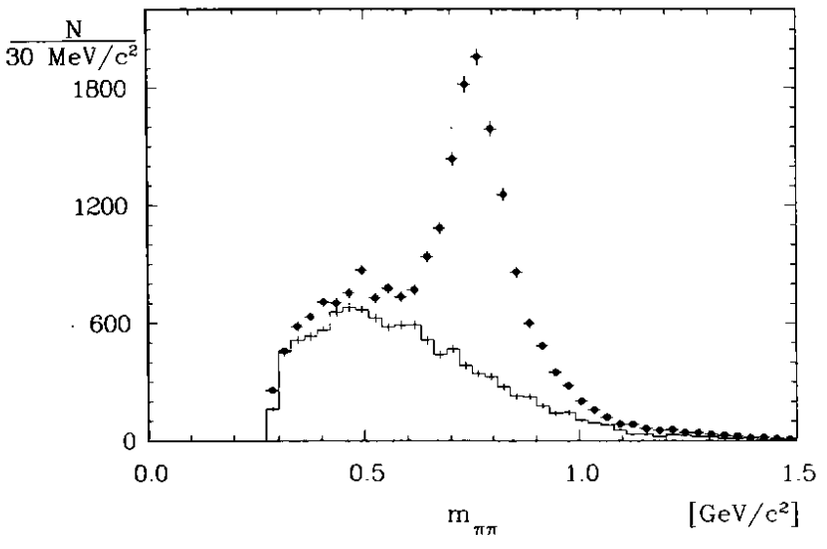

Figure 3

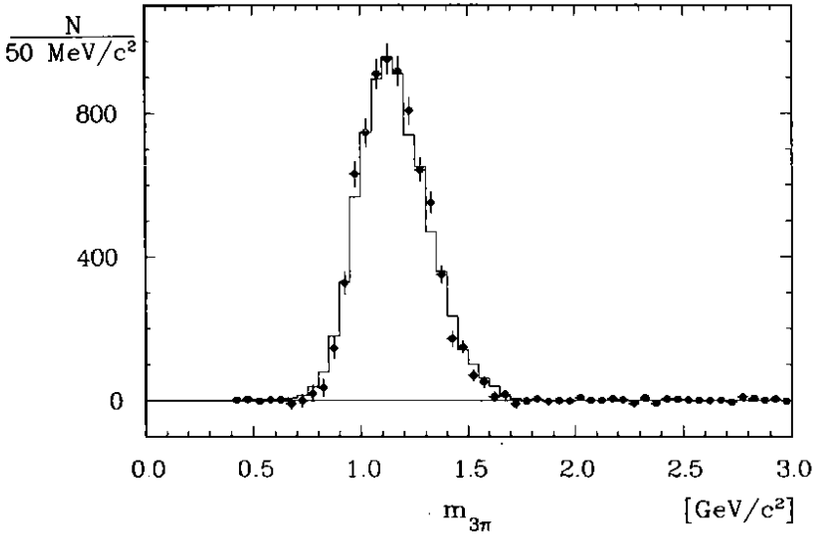

Figure 4

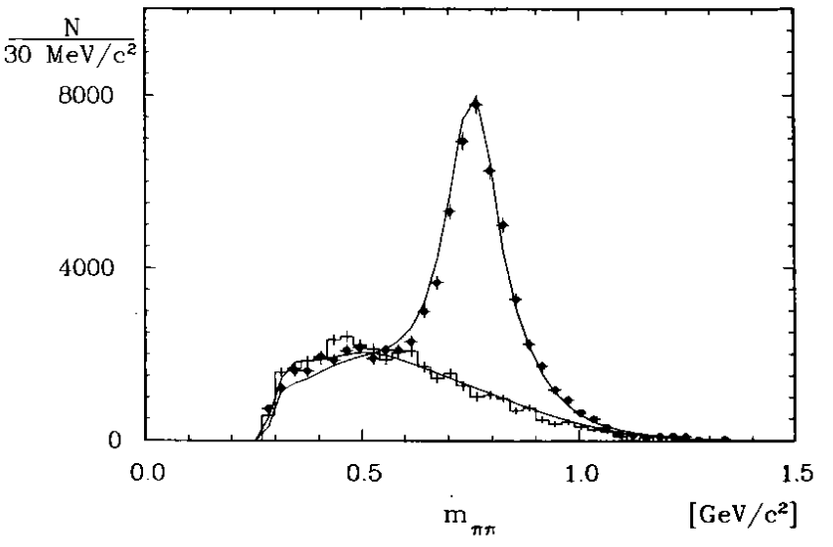

Figure 5

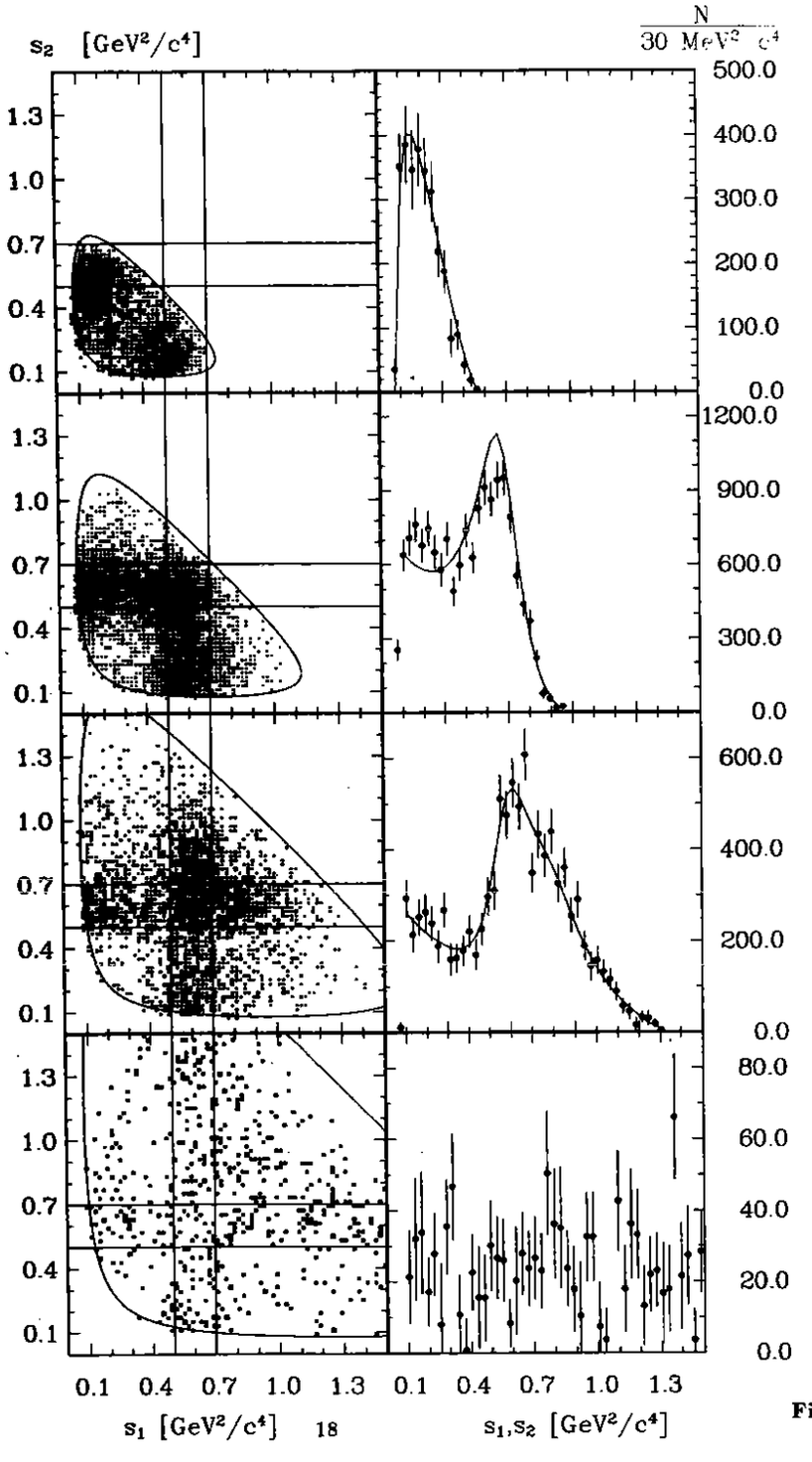

Figure 6

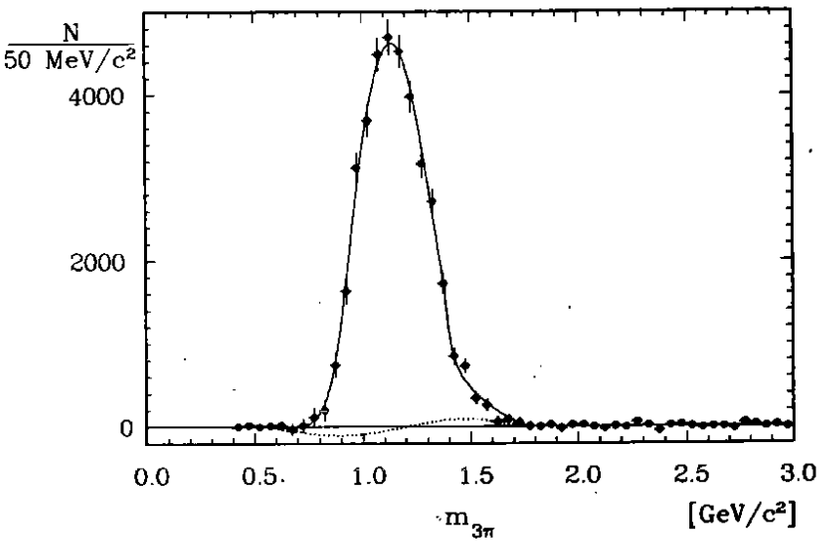

Figure 7

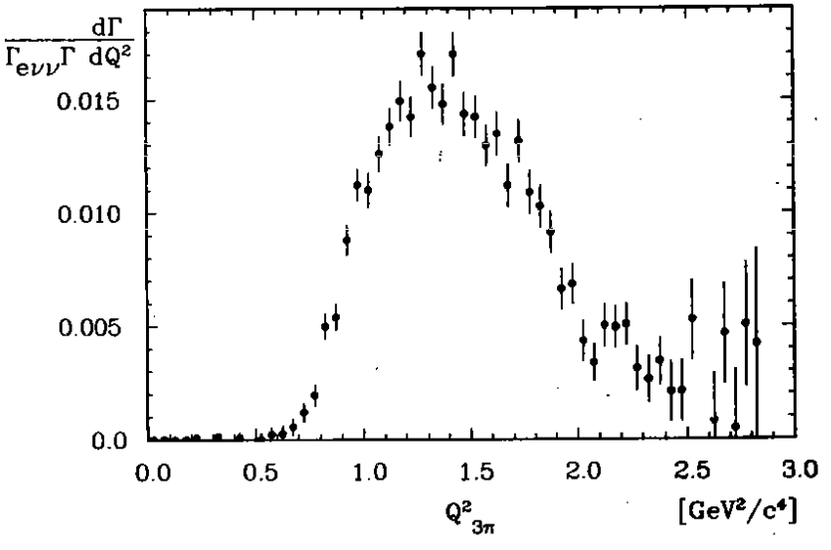

Figure 8

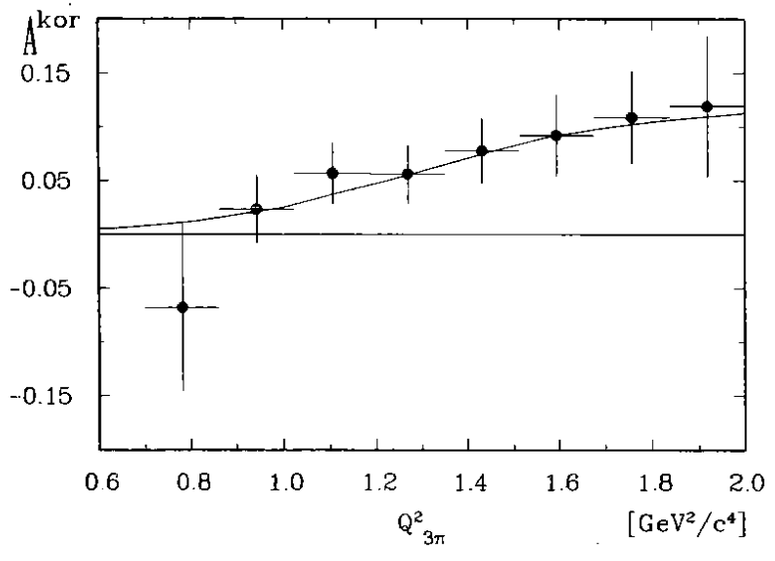

Figure 9

Appendix:

$m_{3\pi}$ GeV/c²	N	$m_{3\pi}$ [GeV/c²]	N
0.425	1 ± 9	1.125	4695 ± 214
0.475	15 ± 16	1.175	4523 ± 198
0.525	−6 ± 28	1.225	3976 ± 187
0.575	11 ± 44	1.275	3167 ± 166
0.625	17 ± 56	1.325	2712 ± 153
0.675	−37 ± 68	1.375	1725 ± 122
0.725	11 ± 89	1.425	850 ± 103
0.775	111 ± 115	1.475	732 ± 84
0.825	196 ± 124	1.525	344 ± 76
0.875	742 ± 146	1.575	258 ± 75
0.925	1635 ± 161	1.625	57 ± 66
0.975	3121 ± 179	1.675	85 ± 60
1.025	3688 ± 196	1.725	48 ± 53
1.075	4489 ± 201	1.775	4 ± 53

Table 5: Background and acceptance corrected three–pion mass distribution.

$Q^2_{3\pi}$ [GeV²/c⁴]	A
0.7813	−0.068 ± 0.078
0.9438	0.023 ± 0.032
1.1062	0.057 ± 0.028
1.2687	0.056 ± 0.027
1.4312	0.078 ± 0.030
1.5937	0.092 ± 0.038
1.7562	0.109 ± 0.043
1.9181	0.119 ± 0.066

Table 6: Parity violating asymmetry as a function of the three–pion mass.

$Q^2_{3\pi}[\mathrm{GeV}^2/c^4]$	$\frac{1}{\Gamma_{e\nu\nu}}\frac{1}{N}\frac{d\Gamma}{dQ^2_{3\pi}}$	$Q^2_{3\pi}[\mathrm{GeV}^2/c^4]$	$\frac{1}{\Gamma_{e\nu\nu}}\frac{1}{N}\frac{d\Gamma}{dQ^2_{3\pi}}$
0.175	0.0002 ± 0.0032	1.625	1.3478 ± 0.0968
0.225	0.0075 ± 0.0058	1.675	1.1191 ± 0.0949
0.275	-0.0039 ± 0.0114	1.725	1.3166 ± 0.0969
0.325	0.0112 ± 0.0167	1.775	1.0888 ± 0.0970
0.375	-0.0054 ± 0.0181	1.825	1.0266 ± 0.0954
0.425	0.0080 ± 0.0218	1.875	0.9109 ± 0.0931
0.475	-0.0377 ± 0.0248	1.925	0.6615 ± 0.0922
0.525	0.0006 ± 0.0287	1.975	0.6831 ± 0.0880
0.575	0.0220 ± 0.0323	2.025	0.4324 ± 0.0889
0.625	0.0241 ± 0.0377	2.075	0.3356 ± 0.0839
0.675	0.0548 ± 0.0375	2.125	0.5009 ± 0.0958
0.725	0.1191 ± 0.0448	2.175	0.4937 ± 0.0931
0.775	0.1944 ± 0.0494	2.225	0.5059 ± 0.0933
0.825	0.4982 ± 0.0564	2.275	0.3111 ± 0.0987
0.875	0.5384 ± 0.0590	2.325	0.2629 ± 0.1049
0.925	0.8795 ± 0.0674	2.375	0.3432 ± 0.1049
0.975	1.1219 ± 0.0715	2.425	0.2082 ± 0.1318
1.025	1.0995 ± 0.0767	2.475	0.2119 ± 0.1372
1.075	1.2602 ± 0.0784	2.525	0.5245 ± 0.1765
1.125	1.3792 ± 0.0809	2.575	-0.1445 ± 0.1698
1.175	1.4935 ± 0.0884	2.625	0.0785 ± 0.2120
1.225	1.4221 ± 0.0887	2.675	0.4643 ± 0.2229
1.275	1.7016 ± 0.0942	2.725	0.0467 ± 0.2596
1.325	1.5515 ± 0.0928	2.775	0.5049 ± 0.2750
1.375	1.4791 ± 0.0930	2.825	0.4194 ± 0.4185
1.425	1.6996 ± 0.0976	2.875	-0.1636 ± 0.4612
1.475	1.4349 ± 0.0974	2.925	-0.3003 ± 0.6370
1.525	1.4231 ± 0.0937	2.975	-0.5640 ± 1.1081
1.575	1.2962 ± 0.0926		

Table 7: a_1 spectral density.